Journal of Medicinal Chemistry

Article

pubs.acs.org/jmc

Optimization of 4-(*N*-Cycloamino)phenylquinazolines as a Novel Class of Tubulin-Polymerization Inhibitors Targeting the Colchicine Site

Xiao-Feng Wang,[†,⊥] Fang Guan,[†] Emika Ohkoshi,[‡] Wanjun Guo,[§] Lili Wang,[†] Dong-Qing Zhu,[†] Sheng-Biao Wang,[†] Li-Ting Wang,[‡] Ernest Hamel,[∥] Dexuan Yang,[§] Linna Li,[§] Keduo Qian,[‡] Susan L. Morris-Natschke,[‡] Shoujun Yuan,[§] Kuo-Hsiung Lee,*[,‡,#] and Lan Xie*[,†]

[†]Beijing Institute of Pharmacology and Toxicology, 27 Tai-Ping Road, Beijing 100850, China

[‡]Natural Products Research Laboratories, UNC Eshelman School of Pharmacy, University of North Carolina at Chapel Hill, North Carolina 27599, United States

[§]Beijing Institute of Radiation Medicine, 27 Tai-Ping Road, Beijing 100850, China

[∥]Screening Technologies Branch, Developmental Therapeutics Program, Division of Cancer Treatment and Diagnosis, National Cancer Institute, Frederick National Laboratory for Cancer Research, National Institutes of Health, Frederick, Maryland 21702, United States

[⊥]Pharmacy Department, Urumqi General Hospital, Lanzhou Military Region, Urumqi 830000, China

[#]Chinese Medicine Research and Development Center, China Medical University and Hospital, Taichung 40402, Taiwan

Ⓢ *Supporting Information*

ABSTRACT: The 6-methoxy-1,2,3,4-tetrahydroquinoline moiety in prior leads 2-chloro- and 2-methyl-4-(6-methoxy-3,4-dihydroquinolin-1(2*H*)-yl)quinazoline (**1a** and **1b**) was modified to produce 4-(*N*-cycloamino)quinazolines (**4a−c** and **5a−m**). The new compounds were evaluated in cytotoxicity and tubulin inhibition assays, resulting in the discovery of new tubulin-polymerization inhibitors. 7-Methoxy-4-(2-methylquinazolin-4-yl)-3,4-dihydroquinoxalin- 2(1*H*)-one (**5f**), the most potent compound, exhibited high in vitro cytotoxic activity (GI_{50} 1.9−3.2 nM), significant potency against tubulin assembly (IC_{50} 0.77 μM), and substantial inhibition of colchicine binding (99% at 5 μM). In mechanism studies, **5f** caused cell arrest in G2/M phase, disrupted microtubule formation, and competed mostly at the colchicine site on tubulin. Compound **5f** and N-methylated analogue **5g** were evaluated in nude mouse MCF7 xenograft models to validate their antitumor activity. Compound **5g** displayed significant in vivo activity (tumor inhibitory rate 51%) at a dose of 4 mg/kg without obvious toxicity, whereas **5f** unexpectedly resulted in toxicity and death at the same dose.

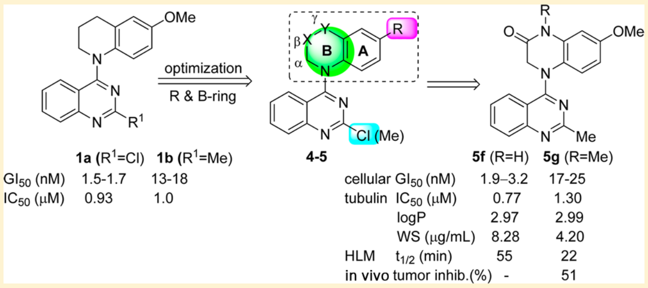

■ INTRODUCTION

Tubulin, a known target of anticancer drugs, has multiple drug-binding sites, the most extensively studied being the taxoid, vinca, and colchicine sites. Colchicine and its analogues (Figure 1) act at a unique site located between the α- and β-tubulin monomers within an αβ heterodimer.[1] These compounds exhibit significant cytotoxicity by inhibiting tubulin polymerization into microtubules, but they are also highly toxic, greatly limiting their clinical use. However, other diverse small molecules that also act at the colchicine site on tubulin have recently come under intensive investigation. These compounds not only potently inhibit the growth of a wide variety of human cancer cell lines but also they show vascular-disrupting effects on tumor endothelial cells required for the growth of the cancer and thus they represent a new class of potential antitumor drugs termed vascular-disrupting agents (VDAs).[2] VDAs can cause a significant shutdown in blood flow to solid tumors by selectively targeting established tumor vasculature, leading to cancer cell death via extensive necrosis and apoptosis while the blood flow in normal tissues remains relatively intact.[3] Therefore, this type of tubulin inhibitor might provide new therapeutic approaches to treat cancers and overcome limitations of existing tubulin-inhibiting drugs. Currently, a dozen drug candidates targeted at the colchicine site are in clinical development as anticancer VDAs[4,5] (e.g., combretastatin A-4 (CA4), its phosphate derivative CA4P,[6] and verubulin (MPC6827)[7]), as shown in Figure 1.

In our prior studies,[8−10] we evaluated a series of *N*-aryl-1,2,3,4-tetrahydroquinoline derivatives and found that lead

Received: October 25, 2013
Published: February 6, 2014

ACS Publications © 2014 American Chemical Society

dx.doi.org/10.1021/jm4016526 | *J. Med. Chem.* 2014, 57, 1390−1402

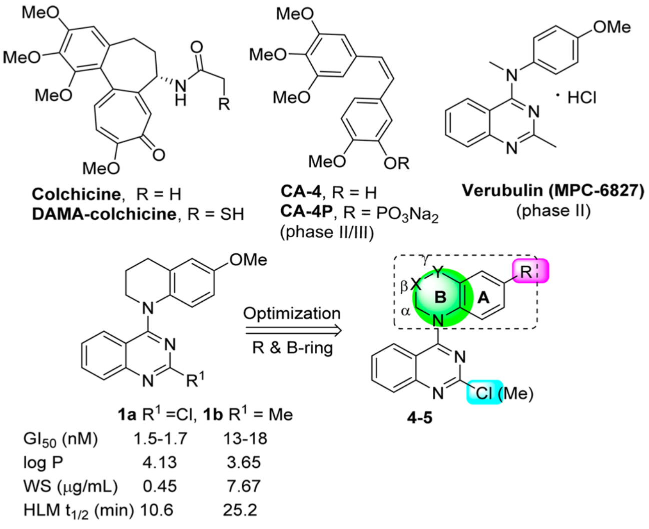

	1a	1b
GI_{50} (nM)	1.5-1.7	13-18
log P	4.13	3.65
WS (μg/mL)	0.45	7.67
HLM $t_{1/2}$ (min)	10.6	25.2

Figure 1. Colchicine, DAMA-colchicine, drug candidates CA4, CA4P, and verubulin, and the modification strategy from leads **1a** and **1b** to new target compounds in this study.

Scheme 1[a]

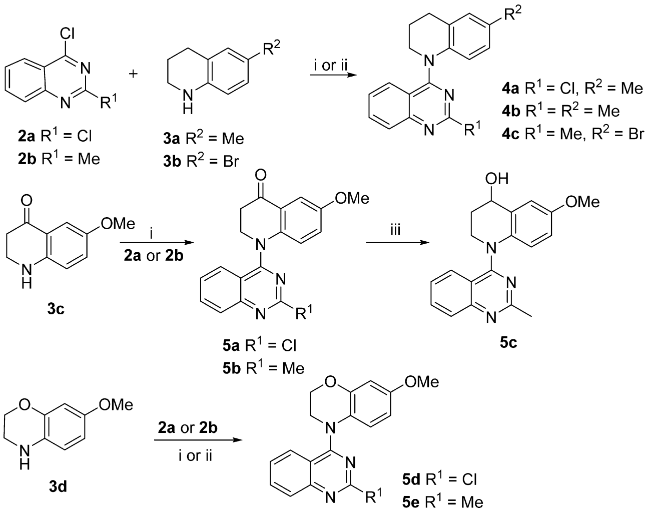

[a] (i) *i*-PrOH/HCl, reflux or rt; (ii) EtOH/$NaHCO_3$, reflux, 1−4 h for **4a** and **5d**; (iii) $NaBH_4$/MeOH, 0 °C to rt.

compounds **1a** and **1b** (Figure 1) exhibited low nanomolar GI_{50} values (1.5−18 nM) against a human tumor cell line (HTCL) panel. Subsequent biological evaluations revealed that, like CA4, **1a** and **1b** inhibited tubulin assembly and colchicine binding to tubulin. These promising results with these new chemotype inhibitors prompted us to elucidate structure−activity relationships (SARs) and structure−property relationships (SPRs) as well as to develop potential new drug candidates. Our modification strategy first focused on the tetrahydroquinoline moiety, as shown in Figure 1. We maintained the quinazolinemoiety because it is a common structural core in various antitumor agents with different targets. These compounds include the tyrosine kinase inhibitor gefitinib,[11] *β*-catenin/Tcf4 inhibitors,[12] and G9a inhibitors.[13] According to the strategy shown in Figure 1, we first changed the R group on the phenyl ring (A-ring) from methoxy to methyl or bromo and determined the effect of these changes on cytotoxic activity. Then, we focused on modifications of the piperidine ring (B-ring) by introducing additional heteroatom(s) or functional groups at the *β* (X) or *γ* (Y) position while maintaining the *α*-methylene group on the B-ring. Next, we changed the B-ring size by reduction to a five-membered ring or expansion to a seven-membered ring. Meanwhile, the 2-substituent on the quinazoline ring was kept as either chloro or methyl, as in leads **1a** and **1b**, respectively. The newly synthesized 4-cycloaminoquinazoline derivatives (**4** and **5**) were evaluated in cellular cytotoxicity and tubulin assays. Further studies on the mechanism of action were performed with the most active compound, **5f**, to identify the biological target of this class of new anticancer agents. Subsequently, several new potent compounds were assessed for essential druglike properties, such as water solubility, log *P*, and in vitro metabolic stability. Finally, antitumor activities of selected compounds with a good balance between potency and physicochemical properties were validated in vivo.

■ CHEMISTRY

The syntheses of new target series **4** and **5** are outlined in Schemes 1−3. Basically, commercially available 2,4-dichloroquinazoline (**2a**) and 4-chloro-2-methylquinazoline (**2b**) underwent nucleophilic substitution with various available or prepared cyclic amines (**3a−h**). As reported previously, the coupling of **2a** with 6-methyl-1,2,3,4-tetrahydroquinoline (**3a**) selectively produced 4-substituted 2-chloroquinazoline **4a** because of the lower reactivity of the C2 as compared with the C4 position.[14] Similarly, **2b** reacted with 6-methyl-1,2,3,4-tetrahydroquinoline (**3a**) or 6-bromo-1,2,3,4-tetrahydroquinoline (**3b**) in the presence of HCl to yield **4b** and **4c**, respectively, in 75−80% yields. 6-Methoxy-2,3-dihydroquinolin-4(1*H*)-one (**3c**)[15,16] and 7-methoxy-3,4-dihydro-2*H*-benzo[*b*][1,4]oxazine (**3d**)[17,18] were prepared according to literature methods and then coupled individually with **2a** and **2b** to afford **5a,b** and **5d,e**, respectively. Next, the ketone in **5b** was converted to the hydroxyl in **5c** by reduction with $NaBH_4$.

In contrast with these simple syntheses, lactam compounds **5f** and **5g** were prepared via multiple steps, as shown in Scheme 2. Commercially available 2-nitro-4-methoxyaniline (**3e**) and **2b** were coupled to provide intermediate diarylamine **6**. Compound **5f** with a new six-membered lactam ring was prepared by a three-step sequence: reduction of the nitro group in **6** by hydrogenation with Pd/C, acylation with 2-chloroacetyl chloride, and subsequent ring closure. Treatment of **5f** with methyl iodide in the presence of NaH afforded N-methylated **5g**.

The syntheses of compounds **5h−i** with a five-membered B-ring and **5j−m** with two different seven-membered B-rings are shown in Scheme 3. 4-Chloroquinazolines **2a** and **2b** were coupled individually with 5-methoxyindoline (**3f**)[19] under alkaline conditions to afford **5h** and **5i**, respectively. In a Schmidt reaction,[20] commercially available 6-methoxy-3,4-dihydronaphthalen-1(2*H*)-one (**9**) was treated with NaN_3 in the presence of CH_3SO_3H to generate a pair of lactam isomers in a ratio of 1:4, which were separated by flash chromatography to give **10a** and **10b**. Compounds **10a** and **10b** were separately reduced with $LiAlH_4$ to afford cyclic amines **3g** and **3h**, respectively, which were coupled with **2a** or **2b** to produce corresponding target compounds **5j−m**, respectively. All newly synthesized compounds were identified by ^1H NMR and MS spectra, and their purities were determined by HPLC.

Scheme 2[a]

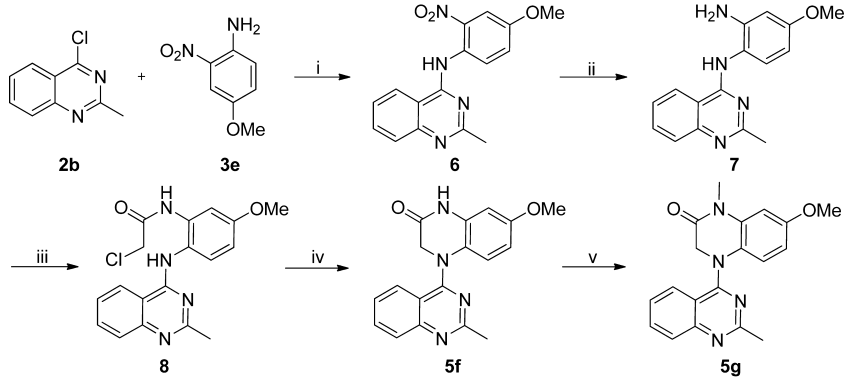

[a](i) *i*-PrOH/HCl, reflux, 5 h, 75%; (ii) H_2/Pd−C, in EtOAc, 2 h; (iii) $ClCH_2COCl$, K_2CO_3, acetone, 0 °C, 1 h, 69% for two steps; (iv) K_2CO_3/DMF, 100 °C, 2 h, 69%; (v) MeI/NaH, DMF, 0 °C, 1 h, 84%.

Scheme 3[a]

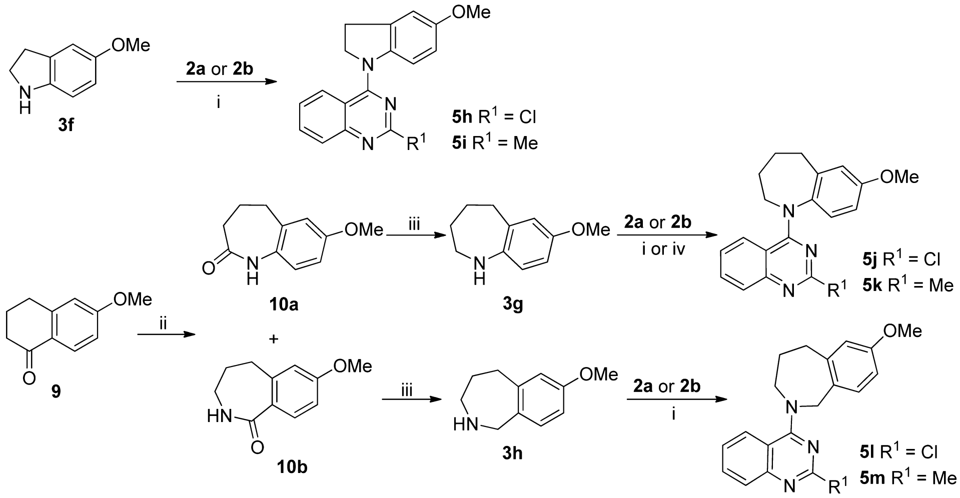

[a](i) $NaHCO_3$, EtOH, rt, 1 h for **5h–i**, or reflux 2 h for **5j** and **5l–m**; (ii) CH_3SO_3H, NaN_3, rt, 24 h; (iii) $LiAlH_4$, THF, reflux, 16 h; (iv) *i*-PrOH/HCl, reflux, 2 h, 64% for **5k**.

RESULTS AND DISCUSSION

Antiproliferative Activity in Cellular Assays and SAR Analysis. Newly synthesized 4-cycloaminoquinazolines (series **4** and **5**) were initially evaluated for antitumor activity against an HTCL panel, including A549 (lung carcinoma), KB (epidermoid carcinoma of the mouth), KBvin, a P-gp-expressing multidrug-resistant cell line (vincristine-resistant KB),[21,22] and DU145 (prostate cancer), in parallel with paclitaxel as a positive reference (Table 1). The in vitro anticancer activity (GI_{50}) was determined using the established sulforhodamine B (SRB) method.[23]

With a 6-methyl or 6-bromo rather than a 6-methoxy (R) group on the A-ring, compounds **4a–c** showed significant cytotoxic activity (GI_{50} 0.043–0.057 μM for **4a** and 0.169–0.211 μM for **4b** and **4c**) but were at least 10-fold less potent than leads **1a** (GI_{50} 1.5–1.7 nM) and **1b** (GI_{50} 0.013–0.018 μM). Thus, the 6-methoxy (R) group is more favorable than methyl or bromo groups.

Next, we focused on modifications of the N-heterocycle (B-ring) in series **5** derivatives. Compounds **5a** and **5b**, with a 4-oxo group added on the tetrahydropyridine B-ring relative to **1a** and **1b**, exhibited high potency with GI_{50} values of 27–33 and 19–24 nM, respectively. Reduction of the carbonyl in **5b** resulted in hydroxyl compound **5c**, which exhibited GI_{50} values of 17–19 nM, similar to those of **5b**. Subsequently, the γ-methylene of the tetrahydropyridine B-ring in **1a** and **1b** was replaced with an oxygen atom. However, the corresponding2*H*-benzo[*b*][1,4]oxazine analogues **5d** and **5e** displayed reduced cytotoxic activity (GI_{50} values of 0.153–0.211 μM). Interestingly, when the tetrahydropyridine B-ring in **1b** was converted to a six-membered lactam ring (3,4-dihydropyrazin-2(1*H*)-one), the resulting 3,4-dihydroquinoxalin-2(1*H*)-one compound (**5f**) showed extremely high cytotoxic activity with low nanomolar GI_{50} values (1.9–3.2 nM), more potent than the positive-control drug paclitaxel against the HTCL panel. The N-methylated lactam (**5g**) also displayed high potency with GI_{50} values of 17–25 nM, although **5g** was less potent than **5f**. However, 5-methoxyindoline compounds **5h** and **5i** with a five-membered 2,3-dihydro-1*H*-pyrrole B-ring showed decreased potency (GI_{50} values of 0.17–0.32 μM) compared with **5a–5g** or leads **1a** and **1b** with various six-membered B-rings. Therefore, the conformational changes and restricted torsional angles of the dihydropyrrole may affect molecular antitumor activity greatly. When the N-heterocyclic B-ring of **1b** was expanded to a seven-membered ring, resulting **5k** with a benzo[*b*]azepine moiety exhibited high potency (GI_{50} values of

Table 1. Antiproliferative Activities of Series 4 and 5 against Human Tumor Cell Lines

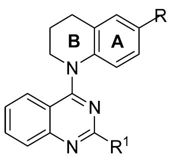

4

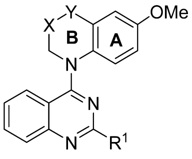

5a-k

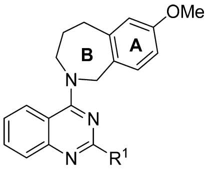

5l-m

compound	R^1	R		GI_{50} (μM ± SD)[a] A549	KB	KBvin	DU145
4a	Cl	Me		0.043 ± 0.011	0.048 ± 0.004	0.046 ± 0.002	0.057 ± 0.011
4b	Me	Me		0.211 ± 0.038	0.204 ± 0.035	0.176 ± 0.031	0.187 ± 0.007
4c	Me	Br		0.211 ± 0.034	0.178 ± 0.028	0.169 ± 0.011	0.198 ± 0.034
compound	R^1	X	Y				
5a	Cl	CH_2	CO	0.027 ± 0.005	0.028 ± 0.005	0.033 ± 0.005	0.031 ± 0.006
5b	Me	CH_2	CO	0.024 ± 0.001	0.019 ± 0.003	0.021 ± 0.001	0.021 ± 0.004
5c	Me	CH_2	CHOH	0.019 ± 0.003	0.018 ± 0.002	0.017 ± 0.001	0.018 ± 0.004
5d	Cl	CH_2	O	0.199 ± 0.004	0.153 ± 0.028	0.195 ± 0.031	0.169 ± 0.021
5e	Me	CH_2	O	0.189 ± 0.016	0.211 ± 0.036	0.169 ± 0.033	0.198 ± 0.033
5f	Me	CO	NH	0.0032 ± 0.0007	0.0023 ± 0.0005	0.0022 ± 0.0004	0.0019 ± 0.0004
5g	Me	CO	NMe	0.019 ± 0.002	0.017 ± 0.003	0.025 ± 0.002	0.022 ± 0.003
5h	Cl	CH_2		0.233 ± 0.013	0.227 ± 0.026	0.197 ± 0.024	0.165 ± 0.035
5i	Me	CH_2		0.268 ± 0.021	0.320 ± 0.056	0.216 ± 0.025	0.243 ± 0.039
5j	Cl	$(CH_2)_2$	CH_2	0.191 ± 0.029	0.227 ± 0.015	0.197 ± 0.024	0.165 ± 0.035
5k	Me	$(CH_2)_2$	CH_2	0.021 ± 0.002	0.019 ± 0.001	0.020 ± 0.001	0.018 ± 0.004
5l	Cl			7.57 ± 0.55	11.30 ± 0.58	5.45 ± 0.90	6.81 ± 1.34
5m	Me			16.71 ± 2.90	19.59 ± 3.33	14.76 ± 2.32	14.63 ± 1.33
paclitaxel[b]				0.0076 ± 0.0017	0.0064 ± 0.0014	1.21 ± 0.19	0.006 ± 0.001

[a] Concentration of compound that inhibits 50% human tumor cell growth, presented as the mean ± standard deviation (SD) and performed at least in triplicate. [b] Positive control.

18–21 nM), similar to the values obtained with **1b**, **5b**, and **5g**. However, the related 2-chloroquinazoline **5j** was much less potent than **5k**. In addition, **5l** and **5m** with the isomericbenzo[*c*]azepine moiety were 300- to 1000-fold less active (GI_{50} 5.45–19.59 μM) than **5k**. Thus, the position of the N atom in the B-ring is important for optimal antitumor activity.

From these results, seven new active 4-aminoquinazoline compounds (**4a**, **5a–c**, **5f–g**, and **5k**) displayed low GI_{50} values ranging from 1.9 to 57 nM (Table 1). Structure–activity relationships conclude that (1) a six-membered or seven-membered B-ring is desirable but the N atom should connect directly to the phenyl ring (A-ring), (2) the six-membered lactam of **5f** and **5g** led to a new favorable chemical scaffold with enhanced cytotoxic activity, and (3) the para-methoxy group (R) on the phenyl ring (A-ring) is more favorable than a methyl or bromo group.

Inhibition of Tubulin Polymerization. Five of the most cytotoxic compounds (**5b-c**, **5f–g**, and **5k**, GI_{50} 1.9–33 nM) were evaluated in tubulin assembly and colchicine binding assays in parallel with CA4, a clinical trial drug candidate, as reference. CA4 is a well-described, highly potent competitive inhibitor of the binding of colchicine to tubulin.[24] The results in these assays are shown in Table 2. Compound **5f**, which displayed the highest cytotoxic potency, also exhibited greater inhibition of tubulin assembly with an IC_{50} value of 0.77 μM and greater potency (99% at 5 μM and 93% at 1 μM) against colchicine binding to tubulin than CA4 (0.96 μM) and leads **1a** and **1b** in the same assays. The other four compounds also showed significant activity in both assays, inhibiting tubulin assembly with IC_{50} values of 0.87–1.3 μM and colchicine binding by 87–96% at 5 μM, similar to CA4 in the same assays. Therefore, these 4-(*N*-cyclo)aminoquinazolines have been identified as a new class of tubulin inhibitors, comparable to our previously discovered *N*-aryl-1,2,3,4-tetrahydroquinolines.

Table 2. Inhibition of Tubulin Polymerization[a] and Colchicine Binding to Tubulin[b]

compound	inhibition of tubulin assembly IC_{50} (μM) ± SD	inhibition of colchicine binding (%) inhibition ± SD 5 μM	1 μM
5b	0.94 ± 0.03	87 ± 1	56 ± 4
5c	0.97 ± 0.1	94 ± 0.7	75 ± 0.6
5f	0.77 ± 0.07	99 ± 0.02	93 ± 0.8
5g	1.3 ± 0.03	96 ± 2	82 ± 0.2
5k	0.87 ± 0.1	89 ± 1	46 ± 0.6
CA4[c]	0.96 ± 0.07	98 ± 0.6	90 ± 0.2

[a] The tubulin assembly assay measured the extent of assembly of 10 μM tubulin after 20 min at 30 °C. [b] Tubulin, 1 μM; [^{3}H]colchicine, 5 μM; and inhibitor, 5 or 1 μM. Incubation was performed for 10 min at 37 °C. [c] The reference compound is a drug candidate in phase II/III clinical trials.

To validate the biological target further, we investigated the effects of the most active compound, **5f**, on the cell cycle. A549 cells were treated with **5f** at 3 nM for 24 h in parallel with colchicine at 300 nM. After staining with propidium iodide, the cells were analyzed by flow cytometry. As shown in Figure 2, cells treated with either colchicine or **5f** were arrested at the G2/M phase, whereas control cells were mainly in the G0/G1 phase. The effects of both compounds on cell cycle distribution patterns were dose-dependent, as shown in Figure 2D.

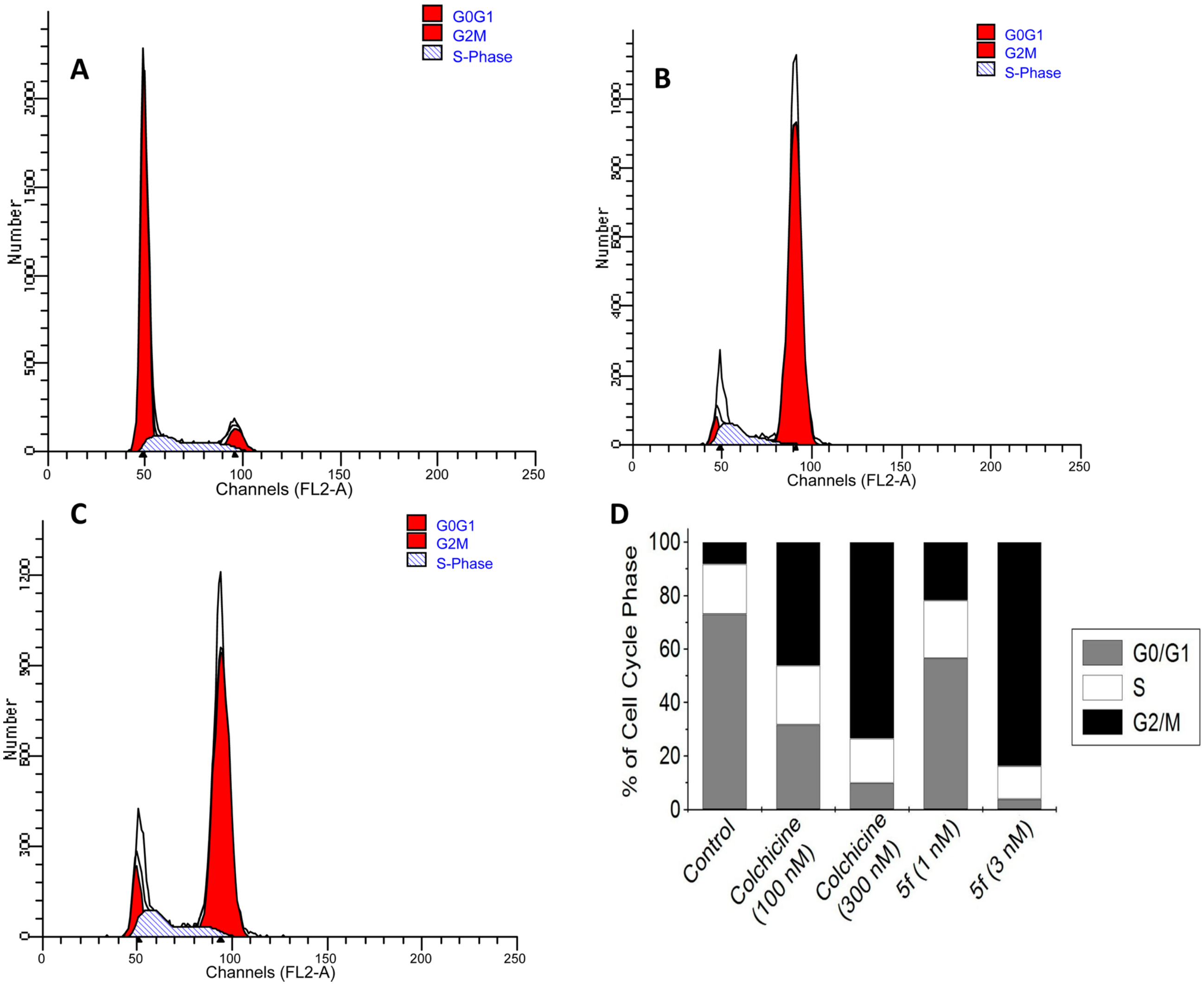

Figure 2. Cell cycle analysis was performed using a FACSCalibur (BD Biosciences) after treatment of A549 cells with **5f** and analysis by a standard propidium iodide procedure as described in the Experimental Section. (A) DMSO-treated (0.1%) cells served as a control. (B, C) A549 cells were harvested after treatment with **5f** (3nM, B) or colchicine (300 nM, C). (D) Cell cycle contributions resulting from treatment with **5f** (1 and 3 nM) or colchicine (100 and 300 nM) for 24 h.

Next, we performed immunocytochemistry studies to examine effects of **5f** treatment on microtubule structure using an α-tubulin antibody to stain cellular microtubules. As shown in Figure 3, a hairlike microtubule network of slim, fibrous microtubules (red) wrapped around the cell nucleus (blue) was visualized upon immunofluorescence staining of A549 cells. However, the microtubule network disappeared when cells were treated with **5f** or colchicine for 24 h (Figure 3B,D), whereas cells treated with paclitaxel retained a spindle-shaped microtubule network around the nucleus.[25] These results indicated that **5f** is unlike paclitaxel as a microtubule-stabilizing agent. To define the actual binding site of **5f** further, competitive assays for the colchicine site or vinblastine site were performed, respectively. We found that compound **5f** decreased the fluorescence intensity of colchicine−tubulin complex in a concentration-dependent fashion with a low IC_{50} value of 0.55 μM, as shown in Figure 4A. In contrast, **5f** did not significantly change the binding of BODIPY FL-vinblastine to tubulin even at 30−100 μM. Vincristine, a vinblastine analogue, did show inhibition in the same assay at 10 μM with inhibition rates of 50−60% (Figure 4B), which is consistent with the literature.[26] Therefore, these results demonstrated that **5f** binds at the colchicine site rather than at the vinblastine site on tubulin.

Molecular Modeling. To elucidate the binding characteristics of these new compounds with tubulin, we performed docking studies with the most active compound, **5f**, at the colchicine binding pocket using the CDOCKER program in the Discovery Studio 3.0 software and the tubulin crystal structure (PDB code: 1SA0)[27,28] in comparison with the original ligand, *N*-deacetyl-*N*-(2-mercaptoacetyl)-colchicine (DAMA-colchicine, Figure 1). As described in our previous publications[8,10] and shown in Figure 5, active compound **5f** (orange stick mode) displayed a binding torsional angle of 66.04° between the two fused rings and a binding conformation with low energy (−39.04 kcal/mol), which superimposed well with DAMA-colchicine (cyan) in the binding site. Like most colchicine-binding inhibitors, key amino acid Cys241 on β-H7 tubulin at the colchicine site forms a hydrogen bond with the methoxy group on the phenyl of **5f**, similar to the 2′-OCH_3 on the A-ring of DAMA-colchicine. It is noteworthy that the carbonyl group in the lactam of **5f** interacts with Leuβ252 and

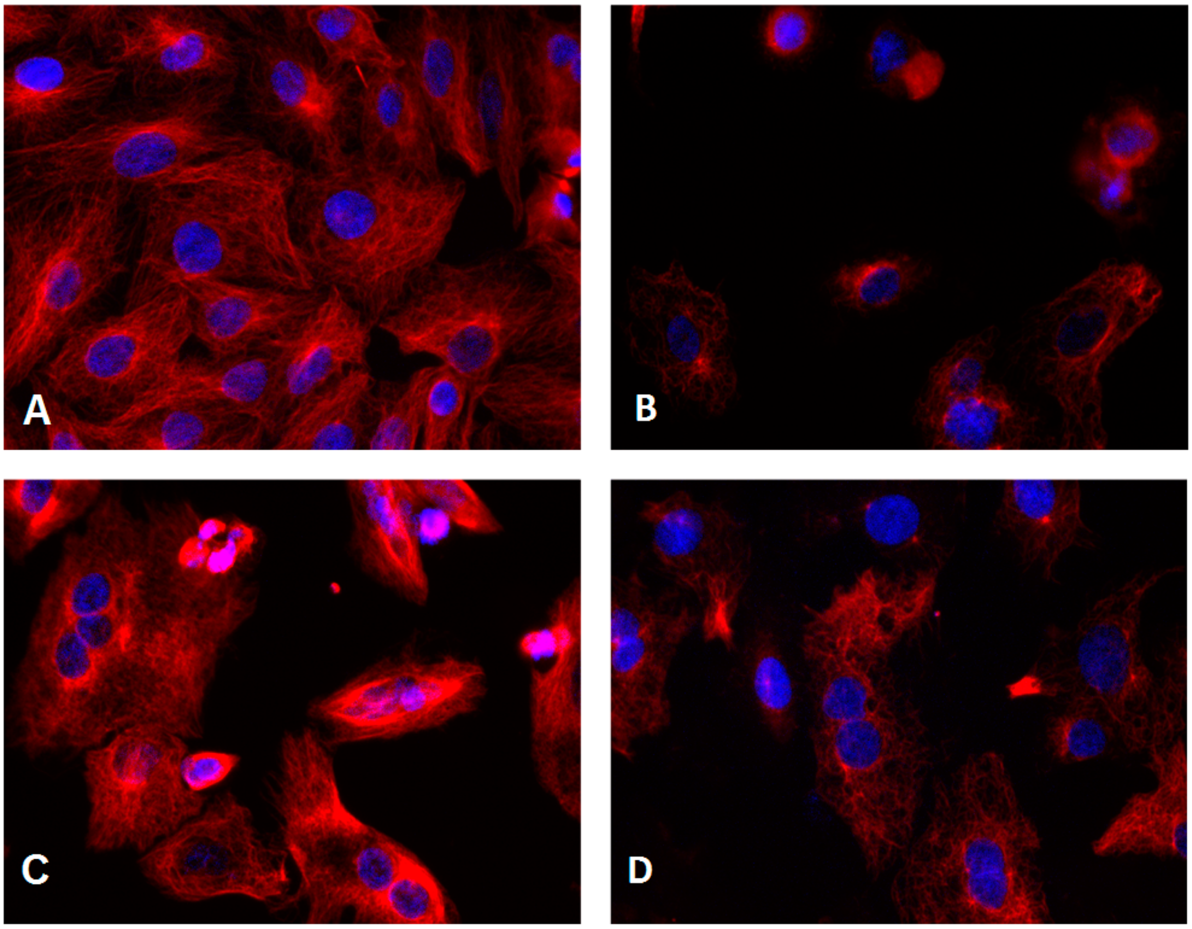

Figure 3. Effects of tested compounds on microtubules. A549 cells were treated with (A) 0.1% DMSO, (B) **5f** (3 nM), (C) paclitaxel (100 nM), or (D) colchicine (100 nM) for 24 h. Microtubules were visualized with an anti-α-tubulin antibody (red), and the cell nucleus was visualized with Hoechst 33342 (blue). Images were acquired with an Incell Analyzer 1000 using a 20× objective.

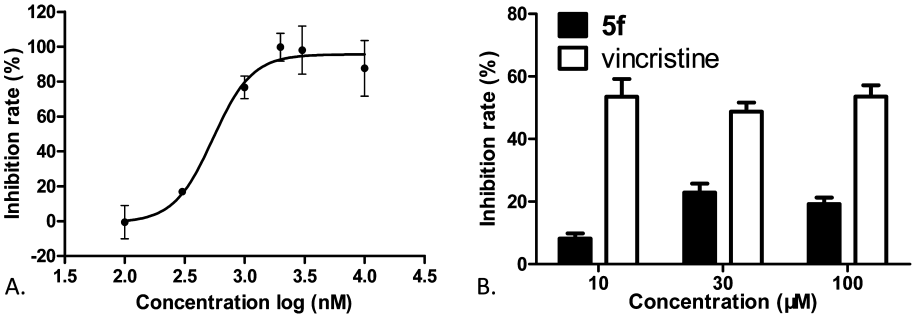

Figure 4. (A) Compound **5f** bound tubulin at the colchicine site. The inhibition curve of **5f** competing with colchicine–tubulin was plotted as inhibition rate vs concentration. The inhibition rates were expressed as the percentage (%) of decreased fluorescence of the tubulin–colchicine complex. An IC_{50} value of 0.55 ± 0.09 μM was determined using GraphPad Prism V5.01. (B) Compound **5f** did not compete for the vinblastine site. Compound **5f** or vincristine at the indicated concentrations competed with BODIPY FL-vinblastine to tubulin. The reduction in the fluorescence intensity of tubulin–BODIPY FL-vinblastine complex was measured and converted into inhibition rates. All results were expressed as the mean ± SD of at least three independent experiments.

Leuβ255 of the β-H8 region of tubulin. The two additional H-bonds could enhance the binding affinity of **5f** with tubulin and subsequently result in the observed higher inhibitory activity on tubulin polymerization. Because the carbonyl group projected deeper into the pocket, the lactam ring (B-ring) of **5f** might have additional hydrophobic interactions with surrounding amino acids. However, the 2-methylquinazoline ring and the phenyl ring of **5f** superimposed well with the two aromatic rings in DAMA-colchicine, suggesting that the two aromatic rings might be important to anchor the ligand at the colchicine-binding pocket and to maintain the required binding conformation. Thus, this modeling investigation provided insight and rationale for the high potency exhibited by **5f** in biological assays (Table 2).

Druglike Properties and Antitumor Activity in Vivo. Prior lead **1b** displayed better druglike properties than **1a** (Figure 1); thus, we chose five active 4-(*N*-cycloamino)phenyl-2-methylquinazolines (**5b–c**, **5f–g**, and **5k**) for assessment of

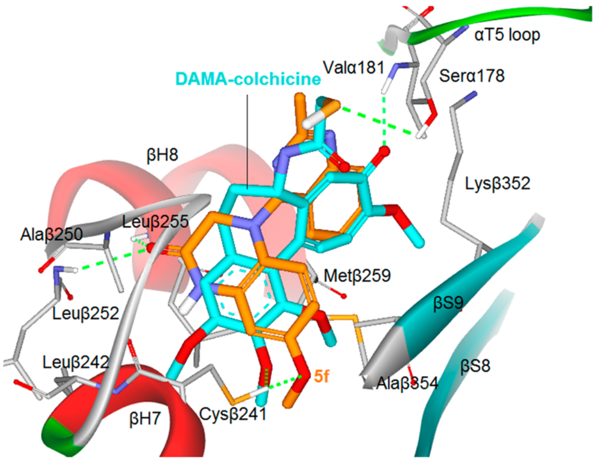

Figure 5. Predicted binding mode of **5f** (orange stick) with tubulin (PDB code: 1SA0) and overlapping with DAMA-colchicine (cyan, the bound ligand of 1SA0). Surrounding amino acid side chains are shown in gray stick format and are labeled. Hydrogen bonds are shown by green dashed lines, and the distance between ligands and protein is less than 3 Å.

essential druglike properties aimed at reaching the critical balance between potency and physicochemical properties required for potential drug candidates. Aqueous solubility, log *P* values, and metabolic stability in a human liver microsome assay were measured according to methods described previously,[29] and data are summarized in Table 3. In comparison, the druglike parameters of most of the new 2-methylquinazoline compounds were better than those of **1a** and similar to those of **1b** (i.e., moderate aqueous solubility (1−10 μg/mL), lower log *P* values (<3, except **5k**), and greater metabolic stability ($t_{1/2}$ 20−55 min, human liver microsome assay)). Among them, the most active compound, lactam **5f**, displayed better metabolic stability in vitro than propranolol ($t_{1/2}$ 54.81 versus 40.82), a drug with moderate metabolic stability. Therefore, we postulate that new compound **5f** might be a good potential drug candidate for further development on the basis of its new structural scaffold, high potency in cellular and tubulin assays, and improved druglike properties.

Table 3. Physicochemical Parameters of Selected Compounds[a]

	pH 7.4		
compound	aqueous solubility (μg/mL)	log *P*	human liver microsome $t_{1/2}$ (min)
1a[b]	0.45 ± 0.06	4.13 ± 0.05	10.59
1b[b]	7.67 ± 0.40	3.65 ± 0.03	25.2
5b	1.21 ± 0.08	2.91 ± 0.05	20.89
5c	8.72 ± 0.13	2.55 ± 0.06	42.44
5f	8.28 ± 0.23	2.97 ± 0.01	54.81
5g	4.20 ± 0.12	2.99 ± 0.03	22.00
5k	2.94 ± 0.11	4.16 ± 0.06	24.85
propranolol[c]			40.82
terfenadine[d]			21.14

[a] Data presented as mean from three separate experiments with or without ± standard deviation (SD). [b] Data reported previously.[10] [c] Propranolol has moderate metabolic stability with $t_{1/2}$ of 3−5 h in vivo. [d] Terfenadine has low metabolic stability with $t_{1/2}$ of <3 h in vivo.

To validate further the antitumor activity in vivo, nude mouse MCF7 xenograft models were established, and compounds **5f**, **5g**, **1a**, and **1b** were administered by intravenous (i.v.) injection at a dose of 4 mg/kg every 3 days. Data are shown in Table 4. Compound **5f** exhibited unexpected toxicity, and all seven mice died during treatment. No obvious signs of toxicity were observed with **5g** at the same dose and schedule. Mice treated with **5g** even had increased body weight after treatment. The higher in vivo toxicity of **5f** might be explained by its better aqueous solubility (Table 3), which should allow **5f** to reach a higher free concentration in blood with less binding to plasma proteins than the more liposoluble **5g** when given by i.v. administration. The result is also consistent with the high antiproliferative activity of **5f** (Table 1). Nevertheless, **5g** significantly inhibited the growth of MCF7 tumor xenografts. Statistically significant differences ($p < 0.05$) compared with the control tumor volumes were reached from day 10 onward (Figure 6A). At the end of treatment, the mice were sacrificed for autopsy, and tumors were recovered and weighed. The average tumor weight of the **5g**-treated group was 0.703 ± 0.323 g, which was much less than that of control mice (1.436 ± 0.531 g), and the tumor growth inhibitory rate was 51.0%. Hence, compound **5g** showed strong antitumor activity on a well-tolerated dose schedule and was more efficacious than **1a** and **1b**.

Table 4. In Vivo Antitumor Data of Compounds 1a, 1b, 5f, and 5g

	administration			toxicity		antitumor activity
compound	dose (mg/kg)	schedule[a]	route	body weight change (%)	death	inhibitory rate (%)
vehicle control		Q3D × 6	i.v.	+0.10	0/7	
1a	4	Q3D × 6	i.v.	−7.9	0/5	22.9
1b	4	Q3D × 6	i.v.	−15.7	1/6	47.3
5f	4	Q3D × 6	i.v.		7/7	
5g	4	Q3D × 6	i.v.	+2.28	0/7	51.0

[a] Q3D, every 3 days.

■ CONCLUSIONS

By structural modifications on the 6-methoxy-1,2,3,4-tetrahydroquinoline moiety in prior leads **1a** and **1b**, a series of 4-(*N*-cycloamino)phenylquinazolines (**4a−c** and **5a−m**) were designed, efficiently synthesized, and evaluated in cellular and tubulin inhibition assays, resulting in the discovery of a new class of antitumor agents as tubulin-polymerization inhibitors. The most potent compound, **5f**, showed low nanomolar antiproliferative activity in cellular assays with GI_{50} values of 1.9−3.2 nM, significant inhibition of tubulin assembly with an IC_{50} value of 0.77 μM, and exceptionally potent inhibition of colchicine binding to tubulin (99% at 5 μM and 93% at 1 μM with colchicine at 5 μM). As a probe in mechanism studies, **5f** arrested most cells in the G2/M phase of the cell cycle and disrupted cellular microtubules, thus providing evidence that these active compounds are a new kind of tubulin-polymerization inhibitors acting at the colchicine site. After druglike property assessments of several active compounds (GI_{50} < 33 nM in the HTCL panel), **5f** and its N-methylated derivative **5g** were evaluated in parallel with **1a** and **1b** in nude mouse MCF7

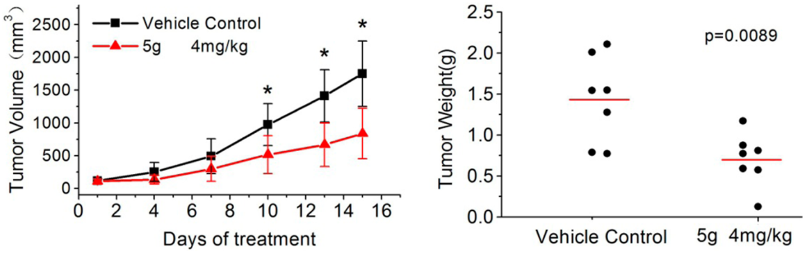

Figure 6. Antitumor activity of **5g** in vivo. MCF7 cells were injected into the flanks of nude mice. When the tumor volume reached about 100 mm^3, the mice were sorted into two groups ($n = 7$) and administration started. (A) Growth difference of tumor volumes was significant from day 10 onward. * indicates a significant difference from control (Student's *t* test, $p < 0.05$). (B) At the end of experiment, tumors were resected and weighed. ● indicates the weight value of each tumor; the red line indicates the average value of the tumor weights.

xenograft models to determine their antitumor activity. Compound **5g** displayed strong in vivo antitumor activity, suppressing tumor growth by 51% at a dose of 4 mg/kg with no obvious signs of toxicity, whereas **5f** resulted in the death of all treated mice on the same dose schedule. SAR studies revealed that (1) the cyclic N-linker (B-ring) can be modified by introducing a polar group at the β and/or γ position to improve activity and physicochemical properties, (2) a suitable torsional angle between the two aromatic rings is important for enhancing molecular affinity for tubulin, (3) the six- or seven-membered cyclic N-linker rings yield active compounds, but the five-membered ring substantially decreased antitumor potency, and (4) the 4-methoxyphenyl ring and the quinazoline moiety are necessary for antitumor activity. Molecular modeling results suggested that the presence of a lactam ring might be responsible for the high potency of **5f** and **5g** by producing additional interactions with the colchicine site on tubulin.

■ EXPERIMENTAL SECTION

Chemistry. The proton nuclear magnetic resonance (^1H NMR) spectra were measured on a JNM-ECA-400 (400 MHz) spectrometer using tetramethylsilane (TMS) as the internal standard. The solvent was $CDCl_3$ unless otherwise indicated. Mass spectra (MS) were measured on an API-150 mass spectrometer with an electrospray ionization source from ABI, Inc. Melting points were measured by a SGW X-4 micro melting-point detector without correction. The microwave (MW) reactions were performed on a MW reactor from Biotage, Inc. Medium-pressure column chromatography was performed using a CombiFlash Companion system from ISCO, Inc. Thin-layer chromatography (TLC) was performed on silica gel GF_{254} plates. Silica gel GF_{254} and H (200−300 mesh) from Qingdao Haiyang Chemical Company were used for TLC and column chromatography, respectively. All commercial chemical reagents were purchased from Beijing Chemical Works or Sigma-Aldrich. Reagents NADPH, $MgCl_2$, KH_2PO_4, and K_2HPO_4 and reference compounds propranolol and terfenadine were purchased from Sigma-Aldrich. HPLC grade acetonitrile for LC−MS analysis was purchased from VWR. Pooled human liver microsomes (lot no. 28831) were purchased from BD Biosciences. Purities of target compounds reached at least 95% and were determined by HPLC using the following instruments and conditions: Agilent HPLC-1200 with UV detector and Agilent Eclipse XDB-C18 column (150 × 4.6 mm, 5 μm), flow rate 0.8 mL/min, UV detection at 254 nm, and injection volume of 15 μL. Mobile elution was conducted with a mixture of solvents A and B (condition 1: acetonitrile (ACN)/H_2O 60:40; condition 2: MeOH/H_2O 70:30). For some compounds, solvent B contained 0.025 mM ammonium acetate.

General Procedure of the Nucleophilic Substitution Reaction for 4a−c, 5a−b, 5d−e, 5h−m, and 6. A solution of 2,4-dichloroquinazoline (**2a**, 0.5 mmol) or 4-chloro-2-methylquinazoline (**2b**, 0.5 mmol) and an amine (0.5 mmol) under condition A (anhydrous *i*-PrOH (5 mL) with a drop of concentrated HCl stirred at rt for 1−12 h or refluxed for 1−5 h) or condition B (in the presence of $NaHCO_3$ (126 mg, 1.5 mmol) in anhydrous EtOH (5 mL) refluxed for 1−4 h). The reaction was monitored by TLC until the reaction was complete. The mixture was poured into ice water and extracted three times with EtOAc. The combined organic phases were washed with water and brine successively and dried over anhydrous Na_2SO_4. After removal of solvent in vacuo, the crude product was purified by flash column chromatography (gradient elution: EtOAc/petroleum ether, 0−70%) to obtain the pure product.

2-Chloro-4-(*N*-(6-methyl-3,4-dihydroquinolinyl))quinazoline (4a). Using condition B starting with **2a** (200 mg, 1.0 mmol) and **3a** (176 mg, 1.2 mmol), the mixture was refluxed for 4 h to produce 248 mg of **4a**: 80% yield, yellow solid, mp 134−136 °C. ^1H NMR δ 2.12 (2H, m, 3′-CH_2), 2.33 (3H, s, CH_3), 2.86 (2H, t, $J = 6.8$ Hz, 4′-CH_2), 4.07 (2H, t, $J = 6.8$ Hz, 2′-CH_2), 6.64 (1H, d, $J = 8.0$ Hz, ArH-8′), 6.78 (1H, dd, $J = 8.4$ and 1.6 Hz, ArH-7′), 7.07 (1H, s, ArH-5′), 7.14 (1H, m, ArH-6), 7.36 (1H, dd, $J = 8.0$ and 0.8 Hz, ArH-5), 7.65 (1H, m, ArH-7), 7.80 (1H, d, $J = 8.0$ and 0.8 Hz, ArH-8). MS *m*/*z* (%) 310 (M + 1, 100), 312 (M + 3, 30). HPLC purity 99.5%.

2-Methyl-4-(*N*-(6-methyl-1,2,3,4-tetrahydroquinolinyl))-quinazoline (4b). Using condition A starting with **2b** (89 mg, 0.5 mmol) and **3a** (74 mg, 0.5 mmol), the mixture was refluxed for 1 h to produce 108 mg of **4b**: 75% yield, yellow solid, mp 136−138 °C. ^1H NMR δ 2.12 (2H, m, 3′-CH_2), 2.30 (3H, s, CH_3), 2.75 (3H, s, CH_3), 2.88 (2H, t, $J = 2.4$ Hz, 4′-CH_2), 4.04 (2H, t, $J = 2.4$ Hz, 2′-CH_2), 6.55 (1H, d, $J = 8.4$ Hz, ArH-8′), 6.73 (1H, dd, $J = 8.4$ and 2.4 Hz, ArH-7′), 7.03 (1H, d, $J = 2.4$ Hz, ArH-5′), 7.13 (1H, m, ArH-6), 7.32 (1H, dd, $J = 8.4$ and 0.8 Hz, ArH-5), 7.63 (1H, m, ArH-7), 7.81 (1H, d, $J = 8.4$ Hz, ArH-8). MS *m*/*z* (%) 290 (M+1, 100). HPLC purity 100.0%.

4-(*N*-(6-Bromo-1,2,3,4-tetrahydroquinolinyl))-2-methylquinazoline (4c). Using condition A starting with **2b** (89 mg, 0.5 mmol) and **3b** (106 mg, 0.5 mmol), the mixture was refluxed for 1 h to produce 142 mg of **4c**: 80% yield, yellow solid, mp 129−130 °C. ^1H NMR δ 2.13 (2H, m, 3′-CH_2), 2.76 (3H, s, CH_3), 2.91 (2H, t, $J = 6.8$ Hz, 4′-CH_2), 4.04 (2H, t, $J = 6.8$ Hz, 2′-CH_2), 6.49 (1H, d, $J = 8.8$ Hz, ArH-8′), 7.01 (1H, dd, $J = 8.8$ and 2.4 Hz, ArH-7′), 7.22 (1H, m, ArH-6), 7.34 (1H, d, $J = 2.4$ Hz, ArH-5′), 7.46 (1H, dd, $J = 8.4$ and 0.8 Hz, ArH-5), 7.69 (1H, m, ArH-7), 7.85 (1H, d, $J = 8.4$ Hz, ArH-8). MS *m*/*z* (%) 354 (M+1, 60), 356 (M+3, 100). HPLC purity 98.1%.

2-Chloro-4-(*N*-(6-methoxy-2,3-dihydro-4-oxoquinolinyl))-quinazoline (5a). Using condition A starting with **2a** (100 mg, 0.5 mmol) and **3c** (89 mg, 0.5 mmol), the mixture was kept at rt for 12 h to produce 61 mg of **5a**: 36% yield, yellow solid, mp 218−220 °C. ^1H NMR δ 2.98 (2H, t, $J = 6.4$ Hz, 3′-CH_2), 3.87 (3H, s, 6′-OCH_3), 4.51 (2H, t, $J = 6.4$ Hz, 2′-CH_2), 6.68 (1H, d, $J = 8.8$ Hz, ArH-8′), 6.88 (1H, dd, $J = 8.8$ and 3.2 Hz, ArH-7′), 7.34 (1H, m, ArH-6), 7.52 (1H, d, $J = 3.2$ Hz, ArH-5′), 7.59 (1H, d, $J = 8.4$ Hz, ArH-5), 7.78 (1H, m, ArH-7), 7.91 (1H, d, $J = 9.2$ Hz, ArH-8). MS *m*/*z* (%) 340 (M + 1, 100), 342 (M + 3, 31). HPLC purity 96.9%.

4-(*N*-(6-Methoxy-2,3-dihydro-4-oxoquinolinyl))-2-methyl-quinazoline (5b). Using condition A starting with **2b** (89 mg, 0.5 mmol) and **3c** (89 mg, 0.5 mmol), the mixture was refluxed for 1 h to produce 109 mg of **5b**: 64% yield, yellow solid, mp 213−214 °C. ^1H NMR δ 2.79 (1H, s, CH_3), 2.97 (2H, t, $J = 6.4$ Hz, 3′-CH_2), 3.85 (3H, s, OCH_3), 4.43 (2H, t, $J = 6.4$ Hz, 2′-CH_2), 6.57 (1H, d, $J = 8.8$ Hz, ArH-8′), 6.84 (1H, dd, *J* = 8.8 and 3.2 Hz, ArH-7′), 7.29 (1H, m, ArH-6), 7.50 (1H, d, *J* = 3.2 Hz, ArH-5′), 7.65 (1H, dd, *J* = 8.4 and 0.8 Hz, ArH-5), 7.75 (1H, m, ArH-7), 7.91 (1H, d, *J* = 8.4 Hz, ArH-8). MS *m/z* (%) 320 (M + 1, 100). HPLC purity 100.0%.

2-Chloro-4-(*N*-(7-methoxy-3,4-dihydro-2*H*-benzo[*b*][1,4]-oxazinyl))quinazoline (5d). Using condition B starting with **2a** (100 mg, 0.5 mmol) and **3d** (91 mg, 0.55 mmol) in EtOH, the mixture was refluxed for 1 h to produce 88 mg of **5d**: 54% yield, yellow solid, mp 173−174 °C. ^{1}H NMR δ 3.79 (3H, s, 7′-OCH_3), 4.23 (2H, t, *J* = 4.8 Hz, 2′-CH_2), 4.51 (2H, t, *J* = 4.8 Hz, 3′-CH_2), 6.31 (1H, dd, *J* = 8.8 and 2.8 Hz, ArH-6′), 6.54 (1H, d, *J* = 2.8 Hz, ArH-8′), 6.72 (1H, d, *J* = 8.8 Hz, ArH-5′), 7.29 (1H, m, ArH-6), 7.73 (1H, m, ArH-7), 7.81 (1H, d, *J* = 8.4 Hz, ArH-5), 7.84 (1H, d, *J* = 8.4 Hz, ArH-8). MS *m/z* (%) 328 (M + 1, 100), 330 (M + 3, 50). HPLC purity 100.0%.

2-Methyl-4-(*N*-(7-methoxy-3,4-dihydro-2*H*-benzo[*b*][1,4]-oxazinyl)quinazoline (5e). Using condition A starting with **2b** (89 mg, 0.5 mmol) and **3d** (83 mg, 0.5 mmol), the mixture was refluxed for 1 h to produce 112 mg of **5e**: 73% yield, yellow solid, mp 139−140 °C. ^{1}H NMR δ 2.73 (3H, s, CH_3), 3.78 (3H, s, OCH_3), 4.17 (2H, t, *J* = 4.4 Hz, 3′-CH_2), 4.50 (2H, t, *J* = 4.4 Hz, 2′-CH_2), 6.28 (1H, dd, *J* = 8.8 and 2.8 Hz, ArH-6′), 6.53 (1H, d, *J* = 2.8 Hz, ArH-8′), 6.67 (1H, d, *J* = 8.8 Hz, ArH-5′), 7.26 (1H, m, ArH-6), 7.71 (1H, m, ArH-7), 7.82 (1H, dd, *J* = 8.4 and 0.8 Hz, ArH-5), 7.85 (1H, d, *J* = 8.4 Hz, ArH-8). MS *m/z* (%) 308 (M + 1, 100). HPLC purity 100.0%.

2-Chloro-4-(*N*-(5-methoxy)indolinyl)quinazoline (5h). Using condition B starting with **2a** (100 mg, 0.5 mmol) and **3f** (75 mg, 0.5 mmol) in anhydrous EtOH (5 mL), the mixture was kept at rt for 1 h to produce 83 mg of **5h**: 53% yield, yellow solid, mp 142−144 °C. ^{1}H NMR δ 3.21 (2H, t, *J* = 8.0 Hz, 3′-CH_2), 3.82 (3H, s, OCH_3), 4.51 (2H, t, *J* = 8.0 Hz, 2′-CH_2), 6.75 (1H, dd, *J* = 8.8 and 2.8 Hz, ArH-6′), 6.86 (1H, d, *J* = 2.8 Hz, ArH-4′), 7.42 (1H, dd, *J* = 8.4 and 1.2 Hz, ArH-6), 7.57 (1H, d, *J* = 8.8 Hz, ArH-7′), 7.76 (1H, dd, *J* = 8.4 and 1.2 Hz, ArH-7), 7.84 (1H, dd, *J* = 8.4 Hz and 1.2 Hz, ArH-5), 8.08 (1H, d, *J* = 8.4 Hz, ArH-8). MS *m/z* (%) 312 (M + 1, 100), 314 (M + 3, 39). HPLC purity 95.1%.

4-(*N*-(5-Methoxy)indolinyl)-2-methylquinazoline (5i). Using condition B starting with **2b** (89 mg, 0.5 mmol) and **3f** (90 mg, 0.6 mmol) in anhydrous EtOH (5 mL), the mixture was kept at rt for 1 h to produce 112 mg of **5i**: 77% yield, yellow solid, mp 116−117 °C. ^{1}H NMR δ 2.70 (3H, s, CH_3), 3.19 (2H, t, *J* = 8.0 Hz, 3′-CH_2), 3.81 (3H, s, OCH_3), 4.45 (2H, t, *J* = 8.0 Hz, 2′-CH_2), 6.69 (1H, dd, *J* = 8.8 and 2.4 Hz, ArH-6′), 6.86 (1H, d, *J* = 2.4 Hz, ArH-4′), 7.37 (2H, m, ArH-7′ and ArH-6), 7.73 (1H, d, *J* = 7.6 Hz, ArH-7), 7.84 (1H, d, *J* = 8.4 Hz, ArH-5), 8.03 (1H, d, *J* = 8.4 Hz, ArH-8). MS *m/z* (%) 292 (M + 1, 100). HPLC purity 100.0%.

2-Chloro-4-(*N*-(7-methoxy-2,3,4,5-tetrahydro-1*H*-benzo[*b*]-azepinyl))quinazoline (5j). Using condition B starting with **2a** (200 mg, 1.0 mmol) and **3g** (177 mg, 1.0 mmol) in anhydrous EtOH, the mixture was refluxed for 2 h to produce 254 mg of **5j**: 75% yield, pale yellow solid, mp 102−103 °C. ^{1}H NMR δ 3.86 (3H, s, OCH_3), 6.68 (1H, dd, *J* = 8.4 and 2.8 Hz, ArH-8′), 6.72 (1H, d, *J* = 8.8 Hz, ArH-5), 6.85 (1H, d, *J* = 8.4 Hz, ArH-9′), 6.92 (1H, d, *J* = 2.8 Hz, ArH-6′), 6.97 (1H, m, ArH-7), 7.54 (1H, m, ArH-6), 7.71 (1H, d, *J* = 8.4 Hz, ArH-8). ^{13}C NMR δ 26.03 (4′C), 28.81 (3′C), 34.27 (5′C), 50.93 (2′C), 55.49 (OCH_3), 112.37 (6′C), 114.97 (8′C), 116.17 (9′C and 10C), 124.88 (8C), 126.07 (11′C), 127.25 (6C), 127.65 (5C), 138.36 (10′C), 141.15 (7′C), 153.37 (9C), 158.98 (2C), 160.92 (4C). MS *m/z* (%) 340 (M + 1, 100), 342 (M + 3, 32). HPLC purity 100.0%.

4-(*N*-(7-Methoxy-2,3,4,5-tetrahydro-1*H*-benzo[*b*]azepinyl))-2-methylquinazoline (5k). Using condition A starting with **2b** (89 mg, 0.5 mmol) and **3g** (88 mg, 0.5 mmol) in *i*-PrOH, the mixture was refluxed for 2 h to produce 206 mg of **5k**: 64% yield, yellow solid, mp 130−131 °C. ^{1}H NMR δ 2.70 (3H, s, CH_3), 3.84 (3H, s, OCH_3), 6.62 (1H, dd, *J* = 8.8 and 2.8 Hz, ArH-8′), 6.77 (2H, m, ArH-5 and 9′), 6.92 (2H, m, ArH-7 and 6′), 7.50 (1H, m, ArH-6), 7.71 (1H, d, *J* = 8.4 Hz, ArH-8). MS *m/z* (%) 320 (M + 1, 100). HPLC purity 98.5%.

2-Chloro-4-(*N*-(7-methoxy-2,3,4,5-tetrahydro-1*H*-benzo[*c*]-azepinyl))quinazoline (5l). Using condition B starting with **2a** (199 mg, 1.0 mmol) and **3h** (177 mg, 1.0 mmol) in EtOH, the mixture was refluxed for 2 h to produce 264 mg of **5l**: 78% yield, yellow solid, mp 159−160 °C. ^{1}H NMR δ 2.17 (2H, m, 4′-CH_2), 3.04 (2H, t, *J* = 1.6 Hz, 5′-CH_2), 3.81 (3H, s, OCH_3), 4.13 (2H, t, *J* = 1.6 Hz, 3′-CH_2), 4.96 (2H, s, 1′-CH_2), 6.77 (2H, m, ArH-6′ and 8′), 7.28 (1H, m, ArH-9′), 7.35 (1H, m, ArH-6), 7.68 (1H, m, ArH-7), 7.76 (1H, d, *J* = 8.4 Hz, ArH-5), 7.93 (1H, d, *J* = 8.4 Hz, ArH-8). MS *m/z* (%) 161 (M−158, 100), 340 (M + 1, 43), 342 (M + 3, 12).

4-(*N*-(7-Methoxy-2,3,4,5-tetrahydro-1*H*-benzo[*c*]azepinyl))-2-methylquinazoline (5m). Using condition B starting with **2b** (178 mg, 1.0 mmol) and **3h** (212 mg, 1.2 mmol) in EtOH, the mixture was refluxed for 2 h to produce 236 mg of **5m**: 74% yield, yellow solid, mp 125−127 °C. ^{1}H NMR δ 2.14 (2H, m, 4′-CH_2), 2.65 (3H, s, CH_3), 3.03 (2H, t, *J* = 5.6 Hz, 5′-CH_2), 3.81 (3H, s, OCH_3), 4.09 (2H, t, *J* = 5.2 Hz, 3′-CH_2), 4.89 (2H, s, 1′-CH_2), 6.73 (1H, dd, *J* = 8.4 and 2.8 Hz, ArH-8′), 6.77 (1H, d, *J* = 2.8 Hz, ArH-6′), 7.24 (1H, d, *J* = 8.4 Hz, ArH-9′), 7.30 (1H, m, ArH-6), 7.65 (1H, m, ArH-7), 7.76 (1H, d, *J* = 8.4 Hz, ArH-5), 7.89 (1H, d, *J* = 8.4 Hz, ArH-8). MS *m/z* (%) 161 (M − 158, 100), 320 (M + 1, 55).

2-Methyl-4-(2-nitro-4-methoxyphenyl)aminoquinazoline (6). Using condition A starting with **2b** (268 mg, 1.5 mmol) and 2-nitro-4-methoxyaniline (**3e**, 278 mg, 1.65 mmol), the mixture was refluxed for 5 h to produce 350 mg of **6**: 75% yield, orange solid, mp 174−175 °C. ^{1}H NMR δ 2.77 (3H, s, CH_3), 3.91 (3H, s, OCH_3), 7.37 (1H, dd, *J* = 9.6 and 3.2 Hz, ArH-5′), 7.06 (1H, t, *J* = 7.6 Hz, ArH-6), 6.62 (1H, d, *J* = 8.8 Hz, ArH-5), 7.77 (1H, d, *J* = 3.2 Hz,ArH-3′), 7.83 (1H, t, *J* = 7.6 Hz, ArH-7), 8.04 (1H, d, *J* = 7.6 Hz, ArH-8), 9.37 (1H, d, *J* = 9.6 Hz, ArH-6′), 11.22 (1H, br s, NH). MS *m/z* (%) 311 (M + 1, 100).

4-(*N*-(4-Hydroxy-6-methoxy-1,2,3,4-tetrahydroquinolinyl))-2-methylquinazoline (5c). To a solution of **5b** (100 mg, 0.31 mmol) in 6 mL of MeOH was added $NaHB_4$ (23 mg, 0.62 mmol) in portions at 0 °C. The mixture was then stirred at rt for another 1 h. After completion of the reaction, the mixture was poured into ice water, neutralized with aqueous HCl (2 N) to pH 6, and extracted three times with EtOAc (20 mL). The combined organic phases were washed with water and brine successively and dried over anhydrous Na_2SO_4 overnight. After removal of solvent in vacuo, the crude product was purified by flash column chromatography (gradient elution: EtOAc/petroleum ether, 0−80%) to give 62 mg of **5c**: 62% yield, yellow solid, mp 136−138 °C. ^{1}H NMR δ 2.13 (1H, m, 3′-CH), 2.37 (1H, m, 3′-CH), 2.74 (3H, s, CH_3), 3.82 (3H, s, OCH_3), 4.00 (1H, m, 2′-CH), 4.21 (1H, m, 2′-CH), 4.94 (1H, m, 4′-CH), 6.60 (1H, dd, *J* = 9.2 and 2.8 Hz, ArH-7′), 6.66 (1H, d, *J* = 9.2 Hz, ArH-8′), 7.06 (1H, s, *J* = 2.8 Hz, ArH-5′), 7.19 (1H, m, ArH-6), 7.50 (1H, d, *J* = 8.4 Hz, ArH-5), 7.67 (1H, m, ArH-7), 7.84 (1H, d, *J* = 8.4 Hz, ArH-8). MS *m/z* (%) 322 (M + 1, 100). HPLC purity 98.8%.

4-(2-Chloroacetylamino-4-methoxyphenyl)amino-2-methyl-quinazoline (8). A mixture of **6** (310 mg, 1.0 mmol) and Pd/C (30 mg, 10% w/w) in 25 mL of EtOAc was stirred under a hydrogen gas atmosphere at rt for 2 h. After removal of the Pd/C by filtration and removal of the solvent in vacuo, the product, 4-(2-amino-4-methoxyphenyl)amino-2-methylquinazoline (260 mg), was dissolved in acetone (20 mL), and K_2CO_3 (386 mg, 2.8 mmol) was added. The mixture was cooled to 0 °C, and chloroacetyl chloride (211 mg, 1.8 mmol) was added dropwise. After addition was complete, the mixture was stirred at the same temperature for 1 h. The mixture was poured into ice water and extracted three times with EtOAc (30 mL). The combined organic phases were washed with water and brine successively and dried over anhydrous Na_2SO_4 overnight. After removal of solvent in vacuo, 264 mg of product **8** was obtained: 69% yield, yellow solid. ^{1}H NMR δ 2.64 (3H, s, CH_3), 3.84 (3H, s, OCH_3), 4.15 (2H, s, CH_2), 6.85 (1H, dd, *J* = 8.4 and 2.8 Hz, ArH-5′), 7.39 (1H, d, *J* = 8.4 Hz, ArH-6′), 7.52 (1H, t, *J* = 7.6 Hz,ArH-5), 7.83 (4H, m, ArH-6, 7, 8, 3′), 9.41 (1H, br s, NH). MS *m/z* (%) 264 (M − 92, 100), 357 (M + 1, 31), 359 (M + 3, 22).

2-Methyl-4-(7-methoxy-2-oxo-3,4-dihydroquinoxalin-4(1*H*)-yl)quinazoline (5f). A mixture of **8** (260 mg, 0.73 mmol) and anhydrous K_2CO_3 (201 mg, 1.46 mmol) in DMF (5 mL) was heated at 100 °C for 2 h. After the reaction was complete, the mixture was poured into ice water, and the precipitated solid was obtained by filtration and dried to give crude product, which was further purified by flash column chromatography (gradient elution: EtOAc/petroleum ether, 0−80%) to afford 161 mg of **5f**: 69% yield, yellow solid, mp 232−233 °C. ^{1}H NMR δ 2.78 (3H, s, 3-CH_2), 3.81 (3H, s, 7-OCH_3), 4.68 (2H, s, 3-CH_2), 6.40 (1H, dd, *J* = 9.2 and 2.8 Hz, ArH-6′), 6.57 (1H, d, *J* = 2.8 Hz, ArH-8′), 6.62 (1H, d, *J* = 9.2 Hz, ArH-5′), 7.22 (1H, m, ArH-6), 7.48 (1H, d, *J* = 8.4 Hz, ArH-5), 7.70 (1H, m, ArH-7), 7.88 (1H, d, *J* = 8.4 Hz, ArH-8), 8.63 (1H, br s, NH). MS *m*/*z* (%) 321 (M + 1, 100). HPLC purity 98.9%.

2-Methyl-4-(1-methyl-7-methoxy-2-oxo-3,4-dihydroquinoxalin-4-yl)quinazoline (5g). To a solution of **5f** (81 mg, 0.25 mmol) and MeI (71 mg, 0.5 mmol) in anhydrous DMF (ca. 3 mL) was slowly added NaH (40 mg, 1.0 mmol, 60% oil suspension) at 0 °C with stirring over about 1 h. When the reaction was complete, as monitored by TLC, the mixture was poured into ice water and extracted with EtOAc three times. After removal of solvent in vacuo, the crude product was purified by flash column chromatography (gradient elution: EtOAc/petroleum ether, 0−70%) to produce 70 mg of **5g**: 84% yield, yellow solid, mp 217−218 °C. ^{1}H NMR δ 2.77 (3H, s, CH_3), 3.48 (3H, s, NCH_3), 3.83 (3H, s, OCH_3), 4.67 (2H, s, CH_2), 6.41 (1H, dd, *J* = 9.2 and 2.8 Hz, ArH-6′), 6.64 (1H, d, *J* = 9.2 Hz, ArH-5′), 6.72 (1H, d, *J* = 2.8 Hz, ArH-8′), 7.20 (1H, m, ArH-7), 7.47 (1H, d, *J* = 8.4 Hz, ArH-5), 7.69 (1H, m, ArH-6), 7.87 (1H, d, J = 8.4 Hz, ArH-8′). MS *m*/*z* (%) 335 (M + 1, 100). HPLC purity 98.8%.

7-Methoxy-4,5-dihydro-1*H*-benzo[*b*]azepin-2(3*H*)-one (10a) and 7-methoxy-2,3,4,5-tetrahydro-1*H*-benzo[*c*]azepin-1-one (10b). To asolution of 6-methoxy-3,4-dihydronaphthalen- 1(2*H*)-one (3.52 g, 20 mmol) in 15 mL of methanesulfonic acid was added NaN_3 (1.69 g, 26 mmol) in portions at 0 °C. The mixture was stirred at rt for 24 h and was then poured into ice water and neutralized with 10% aqueous NaOH to pH 6. The solid was filtered, washed with water, and dried. The crude product was purified by flash column chromatography (gradient elution: EtOAc/petroleum ether, 0−70%) to obtain 0.48 g of **10a** in 13% yield and 1.92 g of **10b** in 50% yield, respectively. Product **10a**: pale yellow solid. ^{1}H NMR δ 2.12 (2H, m, 4-CH_2), 2.33 (2H, t, *J* = 6.8 Hz, 5-CH_2), 2.77 (t, *J* = 7.2 Hz, 3-CH_2),3.81 (3H, s, OCH_3), 6.75 (2H, m, ArH-6, 8), 6.90 (1H, d, *J* = 8.0 Hz, ArH-9), 7.25 (1H, br s, NH). MS *m*/*z* (%)192 (M−21, 100), 214 (M+ 1, 41). Product **10b**: pale yellow solid. ^{1}H NMR δ 2.01 (2H, m, 4-CH_2), 2.85 (2H, t, *J* = 6.8 Hz, 5-CH_2), 3.13 (1H, t, *J* = 6.8 Hz, 3-CH_2), 3.85 (3H, s, OCH_3), 6.22 (1H, br s, NH), 6.72 (1H, d, *J* = 2.8 Hz, ArH-6), 6.85 (1H, dd, *J* = 8.4 and 2.8 Hz, ArH-8), 7.68 (1H, d, *J* = 8.4 Hz, ArH-9). MS *m*/*z* (%) 192 (M − 21, 100), 214 (M + 1, 54).

7-Methoxy-2,3,4,5-tetrahydro-1*H*-benzo[*b*]azepine (3g). A solution of **10a** (328 mg, 1.70 mmol) in THF (10 mL) was added dropwise to $LiAlH_4$ (133 mg, 3.51 mmol, excess) in anhydrous THF (10 mL) at rt under a nitrogen gas atmosphere with stirring followed by reflux for another 16 h. After the reaction was complete, 0.13 mL of water, 0.39 mL of 15% aqueous NaOH, and 0.39 mL of water were added successively to the mixture with stirring for another 10 min at rt. The mixture was filtered through Celite, the solvent was removed in vacuo, and the residue was purified by flash column chromatography (gradient elution: EtOAc/petroleum ether 0−40%) to produce 256 mg of **3g**: 84% yield, brown oil. ^{1}H NMR δ 1.63 (2H, m, 4-CH_2), 1.79 (2H, m, 3-CH_2), 2.74 (2H, m, 5-CH_2), 2.98 (2H, m, 2-CH_2), 3.76 (3H, s, OCH_3), 6.60 (1H, dd, *J* = 8.4 and 2.8 Hz, ArH-8), 6.70 (2H, m, ArH-7, 9). MS *m*/*z* (%) 136 (M − 41, 100), 178 (M + 1, 29).

7-Methoxy-2,3,4,5-tetrahydro-1*H*-benzo[c]azepine (3h). Prepared by the same procedure as **3g** and used directly in the next step without further purification.

Antiproliferative Activity Assay. Target compounds were assayed by the SRB method for cytotoxic activity using a HTCL assay according to procedures described previously.[30−32] The panel of cell lines included human lung carcinoma (A-549), epidermoid carcinoma of the nasopharynx (KB), P-gp-expressing epidermoid carcinoma of the nasopharynx (KBvin), and prostate cancer (DU145). The cytotoxic effects of each compound were expressed as GI_{50} values, which represent the molar drug concentrations required to cause 50% tumor cell growth inhibition.

Tubulin Assays. Tubulin assembly was measured by turbidimetry at 350 nm as described previously.[33] Assay mixtures containing 1.0 mg/mL (10 μM) of tubulin and varying compound concentrations were preincubated for 15 min at 30 °C without guanosine 5′-triphosphate (GTP). The samples were placed on ice, and 0.4 mM GTP was added. Reaction mixtures were transferred to 0 °C cuvettes, and turbidity development was followed for 20 min at 30 °C following a rapid temperature jump. Compound concentrations that inhibited an increase in turbidity by 50% relative to a control sample were determined.

Inhibition of the binding of [^{3}H]colchicine to tubulin was measured as described previously.[34] Incubation of 1.0 μM tubulin with 5.0 μM [^{3}H]colchicine and 5.0 or 1.0 μM inhibitor took place for 10 min at 37 °C, the time at which about 40−60% of maximum colchicine binding occurs in control samples.

Competitive Inhibition Assays. *Colchicine Binding to Tubulin.* Tubulin (4 μM, prepared from fresh dog brain tissue by a literature method[35,36]) in buffer containing 25 mM PIPES (pH 6.8), 1 mM EGTA, and 3 mM $MgCl_2$ was incubated without and with different concentrations (0.1, 0.3, 1, 2, 3, and 10 μM) of **5f** at 37 °C for 45 min in a nontransparent black 96-well plate. Then, colchicine (10 μM) was added to the mixture, which was incubated at 37 °C for an additional 45 min. The fluorescence intensity of the tubulin−colchicine complex (excitation at 340 nm, emission at 435 nm)[37] was measured using a multidetection microplate reader (SpectraMax M5). The inhibition rates of the tested compounds were expressed as the percentage (%) of the decreased fluorescence of the tubulin−colchicine complex. The IC_{50} of **5f** was determined using GraphPad Prism software (V5.01, GraphPad Software Incorporated). Each experiment was performed independently with at least three replicates and expressed as the mean ± SD.

Vinblastine Binding to Tubuline.[26] Tubulin (4 μM) in the same buffer was mixed with **5f** and vincristine at concentrations of 10, 30, and 100 μM, respectively, and incubated at 37 °C. After 30 min, BODIPY FL-vinblastine (2 μM) was added, and the mixtures were incubated for another 30 min. The fluorescence intensity of FL-vin−tubulin complex (excitation at 470 nm, emission at 515 nm) was measured using a multidetection microplate reader (SpectraMax M5). Inhibition rates (%) of the tested compounds were determined by the percent of decreased fluorescence in the same manner as that the colchicine binding to tubulin assay.

Cell Cycle Analysis. A549 cells treated with **5f** (3 nM) or colchicine (300 nM) for 24 h were washed twice in PBS, resuspended in 2 mL of 70% ice-cold EtOH, and kept at 4 °C for 24 h. Fixed cells were washed once in PBS and then treated with 150 μL of a 0.05 mg/mL RNAase solution at 37 °C for 30 min. Cell nuclei were then stained with a PBS solution (150 μL) containing 0.05 mg/mL of propidium iodide for 30 min at rt in the dark. Cell cycle distribution was determined with a FACSCalibur (BD Biosciences).

Immunocytochemistry. A549 cells were grown in black clear-bottom 96-well plates in the presence or absence of tested compounds (**5f**, paclitaxel, or colchicine) for 24 h and fixed in 4% paraformaldehyde for 20 min. After being rinsed with PBS and permeabilized with 0.1% Triton X-100 in PBS for 30 min in the dark, the fixed cells were rinsed again with PBS and blocked with 5% bovine serum albumin (BSA) for 30 min at 37 °C. Then, anti-α-tubulin antibodies (Invitrogen) (1:2000) and the secondary antibody (Alexa Flour 549-donkey anti-mouse IgG; Invitrogen) were added successively to each well and incubated for 2 and 1 h, respectively. Finally, the cells were stained with Hoechst 33342 for 1 h at rt in the dark. Images were acquired by Incell Analyzer 1000 (GE,) using a 20× objective.

Aqueous Solubility Studies. Solubility was measured at pH 7.4 by using an HPLC−UV method. Test compounds were initially dissolved in DMSO at a concentration of 1.0 mg/mL. Ten microliters of this stock solution was added to pH 7.4 phosphate buffer (1.0 mL), with the final DMSO concentration being 1%. The mixture was stirred for 4 h at rt and then centrifuged at 3000 rpm for 10 min. The saturated supernatants were transferred to other vials for analysis by HPLC−UV. Each sample was performed in triplicate. For quantification, a model 1200 HPLC−UV (Agilent) system was used with an Agilent Eclipse XDB-C18 column (150 × 4.6 mm, 5 μm), and elution was with 50−80% ACN in water. The flow rate was 0.8 mL/min, and the injection volume was 20 μL. Aqueous concentration was determined by comparison of the peak area of the saturated solution with a standard curve plotted for the peak area versus known concentrations, which was prepared by solutions of test compound in ACN at 50, 12.5, 3.13, 0.78, and 0.20 μg/mL.

Log *P* Measurements. One to two milligrams of test compound were dissolved in 1.0−2.0 mL of *n*-octane to obtain a 1.0 mg/mL solution. Next, the same volume of water as *n*-octane was added to each vial. The mixture was stirred at rt for 24 h and left without stirring overnight. The aqueous and organic phases of each mixture were transferred to separate vials for HPLC analysis. The instrument and conditions were the same as those for water solubility determinations. The log *P* was calculated by the peak area ratio in *n*-octane and in water.

Microsomal Stability Assay. Stock solutions of test compounds (1 mg/mL) were prepared by dissolving the pure compound in DMSO, and the solutions were stored at 4 °C. Before performing the assay, the stock solution was diluted with ACN to 0.1 mM. For measurement of metabolic stability, all compounds were brought to a final concentration of 1 μM with 0.1 M potassium phosphate buffer at pH 7.4, which contained 0.1 mg/mL of human liver microsomes and 5 mM $MgCl_2$. The incubation volumes were 300 μL, and the reaction temperature was 37 °C. Reactions were started by adding 60 μL of NADPH (final concentration, 1.0 mM) and quenched by adding 600 μL of ice-cold ACN to stop the reaction at 5, 15, 30, and 60 min time points. Samples at the 0 min time point were prepared by adding 600 μL of ice-cold ACN first followed by 60 μL of NADPH. All samples were prepared in duplicate. After quenching, all samples were centrifuged at 12 000 rpm for 5 min at 0 °C. The supernatant was collected, and 20 μL of the supernatant was directly injected into a Shimadzu LC−MS 2010 system with an electrospray ionization source for further analysis. The following controls were also used: (1) positive control incubation containing liver microsomes, NADPH, and reference compound propranolol or terfenadine, (2) negative control incubation omitting NADPH, and (3) baseline control containing only liver microsomes and NADPH. The peak heights of the test compounds at different time points were converted to the percentage of compound remaining, and the peak height values at initial time (0 min) served as 100% values. The slope of the linear regression from log percentage remaining versus incubation time relationships ($-k$) was used to calculate the in vitro half-life ($t_{1/2}$) ($t_{1/2} = 0.693/k$), which was regarded as first-order kinetics. Conversion to in vitro CL_{int} (in units of mL/min/mg of protein) was calculated by the formula CL_{int} = [0.693/(in vitro $t_{1/2}$)][(mL incubation)/(mg of microsomes)]. The HPLC−MS analysis was carried out on a Shimadzu LC−MS 2010 with an electrospray ionization source. An Alltima C18 column (5 μm, 150 × 2.1 mm) was used for HPLC with gradient elution at a flow rate of 0.2 mL/min. The elution conditions were ACN (B) in water (A) at 30% for 0−2 min, 85% for 2−6 min, 100% for 6−9 min, and 30% for 9−12 min. The MS conditions were optimized to a detector voltage of +1.7 kV, with the acquisition mode selected as ion monitoring of the appropriate molecular weights of the test compounds. The curved desolvation line temperature was 250 °C, the heat block temperature was 200 °C, and the neutralizing gas flow was 1.5 L/min. Samples were injected by an autosampler. Electrospray ionization was operated in positive and negative modes.

Antitumor Assay in Vivo. Six-week-old female athymic nude mice (Balb/c nu/nu) were obtained from Vital River and housed under specific pathogen-free conditions in conformity with the Guide for the Care and Use of Laboratory Animals, as adopted and promulgated by Beijing Institute of Radiation Medicine. MCF7 cells (2×10^6) were injected subcutaneously into the right abdominal flanks of the nude mice. Tumor growth was measured with a slide caliper, and volumes were estimated according to the following formula: tumor volume (mm^3) = $L \times W^2 \times 0.5$, where L is length and W is width. When tumor volume reached about 100−300 mm^3, the mice were sorted into a treatment group and a control group with similar mean tumor sizes. The mice in the treatment group received a dose of 4 mg/kg every 3 days by i.v. injection. Control mice were treated the same way, receiving vehicle solution (5% PEG400/PBS) only. The experiment was stopped when the tumor volumes of the control mice reached about 1500 mm^3. At the end of the treatment, the mice were sacrificed for autopsy, and the tumors were recovered and weighed. The tumor growth inhibitory rate was calculated as follows: inhibitory rate (%) = [1− (mean tumor weight of treated group)/(mean tumor weight of control group)] × 100.

Molecular Modeling Studies. All molecular modeling studies were performed with Discovery Studio 3.0 (Accelrys). The crystal structure of tubulin in complex with DAMA-colchicine (PDB code: 1SA0) was downloaded from the RCSB Protein Data Bank (http://www.rcsb.org/pdb) for use in the modeling study. CDOCKER was used to evaluate and predict in silico binding free energy of the inhibitors and for automated docking. The protein protocol was prepared by several operations, including standardization of atom names, insertion of missing atoms in residues and removal of alternate conformations, insertion of missing loop regions based on SEQRES data, optimization of short and medium size loop regions with the Looper algorithm, minimization of remaining loop regions, calculation of p*K*, and protonation of the structure. The receptor model was typed with the CHARMM force field. A binding sphere with a radius of 8.5 Å was defined through the original ligand (DAMA-colchicine) as the binding site for the study. The docking protocol employed total ligand flexibility, and the final ligand conformations were determined by the simulated annealing molecular dynamics search method set to a variable number of trial runs. Docked ligand **5f** was further refined using in situ ligand minimization with the Smart Minimizer algorithm by standard parameters. The ligand and its surrounding residues within the above-defined sphere were allowed to move freely during the minimization, whereas the outer atoms were frozen. The implicit solvent model of Generalized Born with Molecular Volume (GBMV) was also used to calculate the binding energies.

■ ASSOCIATED CONTENT

Ⓢ Supporting Information

HPLC purity data for target compounds and cell cycle assay data. This material is available free of charge via the Internet at http://pubs.acs.org.

■ AUTHOR INFORMATION

Corresponding Authors

*(K.-H.L.) Phone: +1-919-962-0066. Fax: +1-919-966-3893. E-mail: khlee@unc.edu.
*(L.X.) Phone/Fax: +86-10-66931690. E-mail: lanxie4@gmail.com.

Notes

The authors declare no competing financial interest.

■ ACKNOWLEDGMENTS

This investigation was supported by grants 81120108022 and 30930106 from the Natural Science Foundation of China (NSFC) awarded to L.X. and NIH grant CA177584-01 from the National Cancer Institute awarded to K.-H.L. This study was also supported in part by the Taiwan Department of Health, China Medical University Hospital Cancer Research Center of Excellence (DOH100-TD-C-111-005).

■ ABBREVIATIONS USED

CA4, combretastatin A-4; DAMA-colchicine, *N*-deacetyl-*N*-(2-mercaptoacetyl)-colchicine; GBMV, Generalized Born with Molecular Volume; GI_{50}, concentration that inhibits 50% human tumor cell growth; HTCL, human tumor cell line; SAR, structure−activity relationship; SPR, structure−property relationship; VDA, vascular-disrupting agents

REFERENCES

(1) Dumontet, C.; Jordan, M. A. Microtubule-binding agents: A dynamic field of cancer therapeutics. *Nat. Rev. Drug Discovery* **2010**, *9*, 790−803.

(2) Siemann, D. W. The unique characteristics of tumor vasculature and preclinical evidence for its selective disruption by tumor-vascular disrupting agents. *Cancer Treat. Rev.* **2011**, *37*, 63−74.

(3) Tozer, G. M.; Kanthou, C.; Baguley, B. C. Disrupting tumor blood vessels. *Nat. Rev. Cancer* **2005**, *5*, 423−435.

(4) Mason, R. P.; Zhao, D.; Liu, L.; Trawick, M. L.; Pinney, K. G. A perspective on vascular disrupting agents that interact with tubulin: Preclinical tumor imaging and biological assessment. *Integr. Biol.* **2011**, *3*, 375−387.

(5) Wang, X. F.; Xie, L. Vascular disrpting agents targeting at tubulin: A novel class of antitumor drug. *J. Int. Pharm. Res.* **2012**, *39*, 445−454.

(6) Dowlati, A.; Robertson, K.; Cooney, M.; Petros, W. P.; Straford, M.; Jesberger, J.; Rafie, N.; Overmoyer, B.; Makkar, V.; Stambler, B.; Taylor, A.; Waas, J.; Lewin, J. S.; McCrae, K. R.; Remick, S. C. A phase I pharmacokinetic and translational study of the novel vascular targeting agent combretastatin A-4 phophate on a single-dose intravenous schedule in patients with advanced cancer. *Cancer Res.* **2002**, *62*, 3408−3416.

(7) Sirisoma, N.; Pervin, A.; Zhang, H.; Jiang, S.; Willardsen, J. A.; Anderson, M. B.; Mather, G.; Pleiman, C. M.; Kasibhatla, S.; Tseng, B.; Drewe, J.; Cai, S. X. Discovery of *N*-(4-methoxyphenyl)-*N*,2-dimethylquinazolin-4-amine, a potent apoptosis inducer and efficacious anticancer agent with high blood brain barrier penetration. *J. Med. Chem.* **2009**, *52*, 2341−2351.

(8) Wang, X. F.; Tian, X. T.; Ohkoshi, E.; Qin, B. J.; Liu, Y. N.; Wu, P. C.; Hung, H. Y.; Hour, M. J.; Qian, K.; Huang, R.; Bastow, K. F.; Janzen, W. P.; Jin, J.; Morris-Natschke, L. S.; Lee, K. H.; Xie, L. Design and synthesis of diarylamines and diarylethers as cytotoxic antitumor agents. *Bioorg. Med. Chem. Lett.* **2012**, *22*, 6224−6228.

(9) Wang, X. F.; Ohkoshi, E.; Wang, S. B.; Hamel, E.; Bastow, K. F.; Morris-Natschke, S. L.; Lee, K. H.; Xie, L. Synthesis and biological evaluation of *N*-alkyl-*N*-(4-methoxyphenyl)pyridin-2-amines as a new class of tubulin polymerization inhibitors. *Bioorg. Med. Chem.* **2013**, *21*, 632−642.

(10) Wang, X. F.; Wang, S. B.; Ohkoshi, E.; Wang, L. T.; Hamel, E.; Qian, K.; Morris-Natschke, S. L.; Lee, K. H.; Xie, L. *N*-Aryl-6-methoxy-1,2,3,4-tetrahydroquinolines: A novel class of antitumor agents targeting the colchicine site on tubulin. *Eur. J. Med. Chem.* **2013**, *67*, 196−207.

(11) Sordella, R.; Bell, D. W.; Haber, D. A.; Settleman, J. Gefitinib-sensitizing EGFR mutations in lung cancer activate anti-apoptotic pathways. *Science* **2004**, *305*, 1163−1167.

(12) Dehnhardt, C. M.; Venkatesan, A. M.; Chen, Z.; Ayral-Kaloustian, S.; Santos, O. D.; Santos, E. D.; Curran, K.; Follettie, M. T.; Diesl, V.; Lucas, J.; Geng, Y.; DeJoy, S. Q.; Petersen, R.; Chaudhary, I.; Brooijmans, N.; Mansour, T.; Arndt, K.; Chen, L. Design and synthesis of novel diaminoquinazolines with in vivo efficacy for β-catenin/T-cell transcriptional factor 4 pathway inhibition. *J. Med. Chem.* **2010**, *53*, 897−910.

(13) Liu, F.; Barsyte-Lovejoy, D.; Allali-Hassani, A.; He, Y.; Herold, J. M.; Chen, X.; Yates, C. M.; Frye, S. V.; Brown, P. J.; Huang, J.; Vedadi, M.; Arrowsmith, C. H.; Jin, J. Optimization of cellular activity of G9a inhibitors 7-aminoalkoxy-quinazolines. *J. Med. Chem.* **2011**, *54*, 6139−6150.

(14) Smits, R. A.; de Esch, I. J. P.; Zuiderveld, O. P.; Broeker, J.; Sansuk, K.; Guaita, E.; Coruzzi, G.; Adami, M.; Haaksma, E.; Leurs, R. Discovery of quinazolines as histamine H_4 receptor inverse agonists using a scaffold hopping approach. *J. Med. Chem.* **2008**, *51*, 7855−7865.

(15) Takahata, H.; Ohnishi, Y.; Takehara, H.; Tsuritani, K.; Yamazaki, T. A convenient synthesis of monocyclic β-lactams by means of solid-liquid phase transfer reactions. *Chem. Pharm. Bull.* **1981**, *29*, 1063−1068.

(16) Anderson, K. W.; Tepe, J. J. The first intermolecular Friedel−Crafts acylation with β-lactams. *Org. Lett.* **2002**, *4*, 459−461.

(17) Booher, R. N.; Kornfeld, E. C.; Smalstig, E. B.; Clemens, J. A. Synthesis of D-oxa tricyclic partial ergolines as dopamine agonists. *J. Med. Chem.* **1987**, *30*, 580−583.

(18) Iakovou, K.; Kazanis, M.; Vavayannis, A.; Bruni, G.; Romeo, M. R.; Massarelli, P.; Teramoto, S.; Fujiki, H.; Mori, T. Synthesis of oxypropanolamine derivatives of 3,4-dihydro-2H-1,4-benzoxazine, β-adrenergic affinity, inotropic, chronotropic and coronary vasodilating activities. *Eur. J. Med. Chem.* **1999**, *34*, 903−917.

(19) Gangjee, A.; Vasudevan, A.; Queener, S. F. Synthesis and biological evaluation of nonclassical 2,4-diamino-5-methylpyrido[2,3-d]pyrimidines with novel side chain substituents as potential inhibitors of dihydrofolate reductases1. *J. Med. Chem.* **1997**, *40*, 479−485.

(20) Dalence-Guzmán, M. F.; Berglund, M.; Skogvall, S.; Sterner, O. SAR studies of capsazepinoid bronchodilators. Part 1: The importance of the catechol moiety and aspects of the B-ring structure. *Bioorg. Med. Chem.* **2008**, *16*, 2499−2512.

(21) Pérez-Sayáns, M.; Somoza-Martín, J. M.; Barros-Angueira, F.; Diz, P. G.; Rey, J. M. G.; García-García, A. Multidrug resistance in oral squamous cell carcinoma: The role of vacuolar ATPases. *Cancer Lett.* **2010**, *295*, 135−143.

(22) Hung, H. Y.; Ohkoshi, E.; Goto, M.; Bastow, K. F.; Nakagawa-Goto, K.; Lee, K. H. Antitumor agents. 293. Nontoxic dimethyl-4,4′-dimethoxy-5,6,5′,6′-dimethylenedioxybiphenyl-2,2′- dicarboxylate (DDB) analogues chemosensitize multidrug-resistant cancer cells to clinical anticancer drugs. *J. Med. Chem.* **2012**, *55*, 5413−5424.

(23) Rubinstein, L. V.; Shoemaker, R. H.; Paull, K. D.; Simon, R. M.; Tosini, S.; Skehan, P.; Scudiero, D. A.; Monks, A.; Boyd, M. R. Comparison of in vitro anticancer-drug-screening data generated with a tetrazolium assay versus a protein assay against a diverse panel of human tumor cell lines. *J. Natl. Cancer Inst.* **1990**, *82*, 1113−1117.

(24) Lin, C. M.; Ho, H. H.; Pettit, G. R.; Hamel, E. Antimitotic natural products combretastatin A-4 and combretastatin A-2: Studies on the mechanism of their inhibition of the binding of colchicine to tubulin. *Biochemistry* **1989**, *28*, 6984−6991.

(25) Li, P. K.; Pandit, B.; Sackett, D. L.; Hu, Z.; Zink, J.; Zhi, J.; Freeman, D.; Robey, R. W.; Werbovetz, K.; Lewis, A.; Li, C. A Thalidomide analogue with in vitro antiproliferative, antimitotic, and microtubule-stabilizing activities. *Mol. Cancer Ther.* **2006**, *5*, 450−456.

(26) Zhang, Z.; Meng, T.; Yang, N.; Wang, W.; Xiong, B.; Chen, Y.; Ma, L.; Shen, J.; Miao, Z. H.; Ding, J. MT119, a new planar-structured compound, targets the colchicine site of tubulin arresting mitosis and inhibiting tumor cell proliferation. *Int. J. Cancer* **2011**, *129*, 214−224.

(27) Knossow, M.; Jourdain, I.; Lachkar, S. Insight into tubulin regulation from a complex with colchicine and a stathmin-like domain. *Nature* **2004**, *428*, 198−202.

(28) Dorléans, A.; Gigant, B.; Ravelli, R. B. G.; Mailliet, P.; Mikol, V.; Knossow, M. Variations in the colchicine-binding domain provide insight into the structural switch of tubulin. *Proc. Natl. Acad. Sci. U.S.A.* **2009**, *106*, 13775−13779.

(29) Sun, L. Q.; Zhu, L.; Qian, K.; Qin, B.; Huang, L.; Chen, C. H.; Lee, K. H.; Xie, L. Design, synthesis, and preclinical evaluations of novel 4-substituted 1,5-diarylanilines as potent HIV-1 non-nucleoside reverse transcriptase inhibitor (NNRTI) drug candidates. *J. Med. Chem.* **2012**, *55*, 7219−7229.

(30) Boyd, M. R. Status of the NCI preclinical antitumor drug discovery screen. In *Cancer: Principles and Practice of Oncology Updates*; Devita, V. T., Hellman, S., Rosenberg, S. A., Eds.; J. B. Lippincott: Philadelphia, PA, 1989; pp 1−12.

(31) Monks, A.; Scudiero, D.; Skehan, P.; Shoemaker, R.; Paull, K.; Vistica, D.; Hose, C.; Langley, J.; Cronise, P.; Vaigro-Wolff, A.; Gray-Goodrich, M.; Campbell, H.; Mayo, J.; Boyd, M. Feasibility of a high-flux anticancer drug screen using a diverse panel of cultured human tumor cell lines. *J. Natl. Cancer Inst.* **1991**, *83*, 757−766.

(32) Houghton, P.; Fang, R.; Techatanawat, I.; Steventon, G.; Hylands, P. J.; Lee, C. C. The sulphorhodamine (SRB) assay and other approaches to testing plant extracts and derived compounds for activities related to reputed anticancer activity. *Methods* **2007**, *42*, 377−387.

(33) Hamel, E. Evaluation of antimitotic agents by quantitative comparisons of their effects on the polymerization of purified tubulin. *Cell Biochem. Biophys.* **2003**, *38*, 1−22.

(34) Verdier-Pinard, P.; Lai, J.-Y.; Yoo, H.-D.; Yu, J.; Márquez, B.; Nagle, D. G.; Nambu, M.; White, J. D.; Falck, J. R.; Gerwick, W. H.; Day, B. W.; Hamel, E. Structure-activity analysis of the interaction of curacin A, the potent colchicine site antimitotic agent, with tubulin and effects of analogs on the growth of MCF-7 breast cancer cells. *Mol. Pharmacol.* **1998**, *53*, 62−76.

(35) Shelanski, M. L.; Gaskin, F.; Cantor, C. R. Microtubule assembly in the absence of added nucleotides. *Proc. Natl. Acad. Sci. U.S.A.* **1973**, *70*, 765−768.

(36) Hamel, E.; Lin, C. M. Glutamate-induced polymerization of tubulin: Characteristics of the reaction and application to the large-scale purification of tubulin. *Arch. Biochem. Biophys.* **1981**, *209*, 29−40.

(37) Bhattacharyya, B.; Wolff, J. Promotion of fluorescence upon binding of colchicine to tubulin. *Proc. Natl. Acad. Sci. U.S.A.* **1974**, *71*, 2627−2631.